New Insights Into the Role of MADS-box Transcription Factor Gene *CmANR1* on Root and Shoot Development in Chrysanthemum (Chrysanthemum Morifolium)

Cui-Hui Sun
Shandong Agricultural University
Jia-Hui Wang
Shandong Agricultural University
Kai-Di Gu
Sahndong Agricultural University
Peng Zhang
Shandong Agricultural University
Xin-Yi Zhang
Shandong Agricultural University
Cheng-Shu Zheng
Shandong Agricultural University
Fangfang Ma
Shandong Agricultural University
Da-Gang Hu (fap_296566@163.com)
National key laboratory of crop biology https://orcid.org/0000-0002-1443-3646

Research article

Keywords: CmANR1, MADS-box, Root development, Shoot, Metabolomics, Chrysanthemum

Posted Date: November 13th, 2020

DOI: https://doi.org/10.21203/rs.3.rs-104827/v1

Version of Record: A version of this preprint was published at BMC Plant Biology on February 6th, 2021.
See the published version at https://doi.org/10.1186/s12870-021-02860-7.

Abstract

Background: MADS-box transcription factors (TFs) are the key regulators of multiple developmental processes in plants; among them, a chrysanthemum MADS-box TF CmANR1 has been isolated and described as functioning in root development in response to high nitrate concentration signals. However, how CmANR1 affects root and shoot development remains unclear.

Results: We report that CmANR1 plays a positive role in root system development in chrysanthemum throughout the developmental stages of tissue culture. Metabolomics combined with transcriptomics assays show that CmANR1 promotes robust root system development by facilitating nitrate assimilation, and influencing the metabolic pathways of amino acid, glycolysis, and the tricarboxylic acid cycle (TCA) cycle. Also, we found that the expression levels of TFs associated with the nitrate signaling pathways, such as *AGL8*, *AGL21*, and *LBD29*, are significantly up-regulated in *CmANR1*-transgenic plants relative to the wild-type (WT) control; by contrast, the expression levels of *RHD3-LIKE*, *LBD37*, and *GATA23* were significantly down-regulated. These results suggest that these nitrate signaling associated TFs are involved in CmANR1-modulated control of root development. In addition, CmANR1 also acts as a positive regulator to control shoot growth and development.

Conclusions: These findings provide potential mechanisms of MADS-box TF CmANR1 modulation of root and shoot development, which occurs by regulating a series of nitrate signaling associated TFs, and influencing the metabolic pathways of amino acid and glycolysis, as well as TCA cycle and nitrate assimilation.

Highlight

CmANR1 confers pleiotropic positive effects on both root and shoot development in chrysanthemum

Background

Roots are not only essential for water and nutrient uptake, but also for the synthesis of various hormones, organic acids and amino acids in plants [1, 2]. Generally, root growth and development, as well as their responses to changing environmental cues and stressed conditions are usually operated by some complex regulatory networks including molecular components, such as regulatory peptides, small RNAs, and transcription factors (TFs) [3–7]. TFs are particularly crucial for root plasticity and development by regulation of multiple target genes, and their mutation or gain of function might result in dramatic phenotypic modifications responding to the specific conditions [8–10] MADS-box transcription factors are key regulators of multiple developmental processes in plants [11], but their contributions to root development are rarely uncovered. *ANR1*, a MADS-box transcription factor gene, has been reported to play roles in lateral root development under nitrate-rich situations in several plant species, but so far, its underlying regulatory mechanism of root development has been somewhat restricted to unclear auxin-related biological processes in the nitrate signaling pathway [12]. Moreover, there is little evidence to

support its roles in shoot development, in addition to its roles in root development [13, 14]. Therefore, at present, to connect *ANR1* to both root and shoot development has become a new challenge.

Omics analysis has become a widespread tool for identifying relevant biomarkers by measuring the content of biochemicals associated with the action modes at the level of DNA/RNA, metabolites, and proteins [15]. High-throughput transcriptome sequencing has been widely applied for the efficient and comprehensive analysis of molecular mechanisms by discovering differently expressed genes (DEGs) in different organs, tissues and cultivars under some specific conditions [16]. Metabolomics is now increasingly used for identifying potential biomarkers, and exploring networks in organisms under environmental or genetic perturbations [17, 18]. Sometimes, metabolomics combined with transcriptomics or proteomics, referred to as integrated metabolomics or metatranscriptomics, is suited for understanding the metabolism under phenotype of genome function via 'gene-metabolism-phenotype' research model [19, 20]. Ultra-high performance liquid chromatography-quadruple time-of-flight mass spectrometry (UPLC-QTOF-MS) and HPLC-ESI have been widely used in plant metabolomic studies. These data provide accurate measurements of vast metabolites and can facilitate the study of complex trait regulation [21–23].

Due to the significant correlation between morphological traits and metabolites in plants, in this study, six samples of *CmANR1*-transgenic and wild-type (WT) (six samples of each) chrysanthemum, respectively, were used for metabolite profiling of roots and shoots. The non-targeted UPLC-QTOFMS-based and GC-MS-based metabolomics analyses were applied to screen for the differently accumulated metabolites in transgenic chrysanthemum relative to its wild type. The metabolomic analysis together with the previous transcriptomic analysis of roots revealed new possible mechanisms underlying the regulation of *CmANR1* on root development in chrysanthemum. Meanwhile, the metabolite profiling results of both roots and shoots of *CmANR1*-transgenic and WT plants indicated that in the *CmANR*1-overexpressing background and *CmANR1*-nitrate signaling dependent condition, there were significant increases of metabolites involved in various amino acid metabolism and carbohydrate digestion and absorption in roots. Meanwhile, the metabolites relevant to amino acid metabolism, such as asparagine and histidine were decreased, and the main metabolites in connection with unsaturated/fatty acids biosynthesis were increased in the shoots of transgenic plants. Moreover, positive effects on shoot development were confirmed in transgenic plants, with a longer shoot and better photosynthetic performance than those of WT plants, suggesting that CmANR1 might exert pleiotropic effects on root and shoot development in chrysanthemum.

Results

CmANR1 plays a positive role in root development in chrysanthemum throughout the developmental stage of tissue cultures

Three independent *CmANR1*-transgenic lines (*CmANR1-OVX56*, *-OVX67*, and *-OVX81*) of chrysanthemum were generated by introducing a *35S::CmANR1-GFP* vector into chrysanthemum leaf discs via

Agrobacterium GV3101 [24] (Fig. 1a). The *CmANR1*-transgenic plants displayed a more forceful growth potency on root development in comparison to the WT plants at the early stage of tissue culture growth (10 day-olds) (Fig. 1b). The numbers of the adventitious root (AR) in *CmANR1*-OVXs lines were significantly increased by 23.8–69.3% compared to the WT plants (Fig. 1c). Meanwhile, a significant increase in the length of the root was detected in transgenic plants compared to the WT plants, as suggested by the length distribution of ARs and root hairs (Fig. 1d). Interestingly, electron microscope observation showed that the number and length of root hairs in the *CmANR1*-OVXs lines were also obviously improved relative to the WT plants (Fig. 1e-g). These results suggest that CmANR1 plays a positive role in root development in chrysanthemum at the early stage of tissue culture growth.

Here, we show that CmANR1 positively modulates root system development and is involved in both AR and lateral root at later stage (40 days old) of tissue cultures growth. Therefore, it seems that CmANR1 positively controls root system development throughout the developmental stage of tissue cultures.

Metabolite profiling of roots in both CmANR1-overexpressing and WT chrysanthemum by UHPLC-Q-TOF/MS

The intermediates and its final biochemical products at tissue level are closely related to genotypes, and might directly affect complex quantitative traits in plants [18]. Therefore, identifying the differently accumulated metabolites in roots between transgenic and WT plants might better decipher the underlying regulatory mechanism of *CmANR1* on root development. Thus, the metabolite profiling of roots in both *CmANR1*-overexpressing (*CmANR1*-OVXs) and WT chrysanthemum was tested by ultra-high-performance liquid chromatography-tandem quadrupole/time-of-flight mass spectrometry (UHPLC-Q-TOF/MS). Quality control (QC) samples were regarded as the representative “mean” sample, including all analytes during the analysis and were handled as real samples in the ESI positive or negative analysis batch to monitor the stability of the instrument [25]. Principal component analysis (PCA), partial least squares discrimination analysis (PLS-DA), and orthogonal projections to latent structures discriminant analysis (OPLS-DA) were carried out using the retention peaks on all the samples from the study, including conditioning runs and QC samples. All of the QC samples (Blue) were clustered tightly in PCA score plots (Additional file 1). The consistency of the repeated QCs and the reliable data quality of all the experimental samples support the credibility of the method for metabolite profiling in this study.

A total of 3,194 and 2,927 retention peaks, in positive and negative mode, respectively, were extracted from all the samples using XCMS software. PCA score plots in ESI positive and negative mode revealed a trend of separation between the transgenic and WT samples (Fig. 2a, b). In the OPLS-DA modeling analysis, the evaluation parameter R2Y and Q2 $\geq$ 0.5, which indicated that the analytical method was robust with good stability and reliability in this study (Additional file 2). Meanwhile, variable importance for the projection (VIP) based on the OPLS-DA model could be used to evaluate the expression pattern of each metabolite on the classification discrimination and the explanatory ability of each group of

samples, and to explore differential metabolites of biological significance. Using VIP > 1 as the screening standard, differently accumulated metabolites were preliminarily selected in the root samples of *CmANR1*-OVXs and WT chrysanthemum (Table 1). These metabolites were roughly divided into three categories: amino acids, carbohydrates, and alkaloids (Table 1). Metabolites regarding to various amino acid biosynthesis and metabolism, TCA cycle and pentose metabolism, as well as pyrimidine, vitamin B6 metabolism, were altered when *CmANR1*-OVXs and WT plants were compared. Moreover, hierarchical clustering analysis was performed based on the degree of similarity of the significant metabolite abundance profiles in roots. Metabolites with similar expression patterns were clustered together, which indicates their involvement in the relatively close reaction steps of the metabolism processes. For instance, L-histidine and 4-guanidinobutyric acid were clustered together, confirming their roles in amino acid metabolism. Similarly, citrate, maltotriose and D-mannose were closely clustered, indicating their possible actions in glycometabolism (Fig. 2c, d).

CmANR1 promotes roots system development by facilitating nitrate assimilation

It is well known that nitrate is not only the primary source of nitrogen for most of the higher plants, but also acts as a signal to regulate global genes expression and many physiological processes in plants [26, 27]. In addition, we have proved that CmANR1 promotes lateral and adventitious roots development in response to higher environmental nitrate concentration signals by altering its trans-activation activity of auxin transport genes in chrysanthemum [28]. Accordingly, the nitrate content in the roots of *CmANR1*-overexpressing chrysanthemum was higher in the WT control, with an increase of 25.5%, 27.6%, and 13.6% (Fig. 3a). A quantitative real-time PCR (qRT-PCR) assay showed that the expression of several nitrate transporter genes, such as *NRT1.2*, *NPF5.2*, *NPF8.3*, was significantly increased in transgenic plants (Fig. 3b), which can account for increase of nitrate content in the roots of *CmANR1*-OVXs chrysanthemum. Additionally, several genes encoding nitrate reductase (TR16877|c0_g8, -0.772337; TR16877|c0_g9, -3.56766), nitrite reductase (TR7757|c0_g2, -1.05013), and GOGAT (TR9225|c1_g1, 1.373529) that are involved in nitrate assimilation processes showed significantly differential expression in comparison of *CmANR1*-transgenic and WT plants (Fig. 3c). Notably, the root metabolites profiling data showed that several amino acids were differently accumulated in comparison between *CmANR1*-transgenic and WT plants. Four important biomarkers in amino acid metabolism (L-histidine, L-pyroglutamic acid, L-citrulline, and phenylacetylglycine) were increased by 4.10-, 2.49-, 2.05-, and 1.80-fold, respectively, in a ratio of *CmANR1*-OVXs/WT. However, L-glutamine and L-phenylalanine showed changes of 0.75 and 0.54 folds when we compared *CmANR1*-OVXs to WT (Table 1). Once nitrate is transported into cells, it undergoes assimilation and is converted into amnio acids that go on taking part in many physiological processes in roots. Therefore, we propose that CmANR1 promotes roots system development by facilitating nitrate assimilation based on the nitrate content increase, as well as the changes of amino acid content in the roots of transgenic plants.

CmANR1 influences the metabolic pathways of glycolysis and TCA cycle during root development in chrysanthemum

Our previous transcriptome sequencing was performed with the roots of *CmANR1*-OVXs and WT chrysanthemum, which provided us with much information about the molecular mechanism of *CmANR1* in root development [24]. To further explore more possibilities of the regulatory mechanism of *CmANR1* in roots, we carried out a metatranscriptomic analysis of roots in *CmANR1*-OVXs and WT chrysanthemum. The Venn diagram showed 36 significant differential transcripts and metabolites were involved in the same metabolic pathway (Fig. 4a). Surprisingly, during the top10 KEGG pathways shared by the two omics, the transcripts involving in 'Amino sugar and nucleotide sugar metabolism' were best represented (Fig. 4b; Additional file 4). Then, we listed several representative sugar metabolic pathways in this term and found that the expression of the genes encoding key enzymes in these sugar metabolism pathways was significantly altered in *CmANR1*-transgenic plants. For example, the genes encoding chitinase (TR4985|c0-g1), hexokinase (TR12735|c0-g1), frutokinase (TR12776|c5-g3), and UDP-glucose 4,6-dehydratase (TR21678|c0-g1, TR21678|c0-g4) showed obvious expression differences between *CmANR1*-transgenic and WT plants (Fig. 4c). Moreover, two main metabolites, citrate and malate were significantly accumulated and relative genes were significantly up-regulated and down-regulated during in glycolysis and TCA cycle in the roots of *CmANR1*-OVXs compared to those of WT plants (Fig. 4d), suggesting that CmANR1 might somehow affect glycolysis and the TCA cycle in the roots of transgenic plants. Afterward, these changes during the active biochemical processes might provide more carbon skeletons for the biosynthesis of other metabolites, and more energy equivalents for some physiological processes, facilitating root system development in chrysanthemum.

Nitrate signaling associated TFs are involved in CmANR1-modulated control of root development

At present, we have clarified two mechanisms, the motivation of nitrate assimilation and possible glycolysis and TCA cycle-related facilitating effect, under the regulation of *CmANR1* on root development in chrysanthemum. However, the exact mechanisms underlying the regulation of *CmANR1* are far more complicated. Transcription factors are important upstream regulators and play critical roles in a wide range of physiological processes in plants. In our previous transcriptome sequencing data, a total of 1,752 DEGs encoding inscription factors (TFs) were identified and could be classified into about 34 main different families (Fig. 5a). Apart from a set of very small share families that we named as 'The other kind', the largest group of differently expressed transcription factor genes was the bHLH family (176, 10.48%), followed by the NAC (141, 8.40%), ERF (116, 6.91%), WRKY (110, 6.55%), MYB-related (99, 5.90%), MYB (83, 4.94%), and C2H2 (68, 4.05%) families. Notably, the LBD (49, 2.31%), M-type_MADS (38, 2.26%), and TCP (18, 1.07%) families were also occupied a certain proportion (Fig. 5b). Members of these three TF families were deemed to be the most relevant to lateral root development as well as nitrate signaling pathway [11, 29, 30], which was in good accordance with our study background. Then, we selected and drew a heat map of several TF genes from the above-mentioned TF families that have been

reported to regulate root or root hair development in other plant species [31–34]. For example, the heat map showed that the expression levels of *AGL8*, *ERF3*, *AGL21*, *LBD29*, and *NLP6* were significantly up-regulated in *CmANR1*-transgenic plants compared to WT plants, while the expressions of *RHD3-LIKE*, *LBD37* and *GATA23* were significantly down-regulated (Fig. 5c). Furthermore, the result of real-time PCR assays of several selected genes related to LR or hair root development was in agreement with the RNA-seq analysis, confirming the validity of the RNA-seq data (Fig. 5d). The expression changes of these genes, on the one hand, suggest their possible correlation with LR or root hair development under the molecular regulation of *CmANR1* in chrysanthemum. On the other hand, the numerous differently expressed TF genes between transgenic and WT plants hint at the complexity of root development under the nitrate treatment conditions.

CmANR1 acts as a positive regulator to control shoot growth and development in chrysanthemum

At one time, more concerns were focused on defining the role of *ANR1* in root development, such as its positive regulation of LR initiation and LR length in *Arabidopsis and* chrysanthemum [28, 35, 36], as well as its promotion on LR and PR development in a nitrate-dependent manner in rice [13]. In fact, we found that the shoots of *CmANR1*-transgenic plants exhibited more vigorous growth in the early tissue-cultured period than the shoots of WT plants (Fig. 1a). This phenomenon continued throughout the culture period. We measured the shoot growth of the tissue-cultured plants. The shoots of transgenic plants were higher than those of WT plants, with an increase from 55.3–97.3% (Fig. 6a). More nodes were observed on shoots of transgenic plants (Fig. 6b), which was a reason for the longer shoot. However, the longer internode length was not ruled out in transgenic plants, because the shoot length of *CmANR1*-OVXs was significantly higher than that of WT plants, even though some transgenic plants (*CmANR1*-OVX56, OVX81) indeed showed no obvious advantage on node number (Fig. 6c). Also, we carried out detailed studies on chlorophyll content and photosynthetic properties of leaves on these plants. The chlorophyll content level in transgenic plants was much higher than that of WT plants (Fig. 6d). And the latter measurements on actual photochemical efficiency (ΦPSII), net photosynthetic rate (Pn), and electron transfer rate (ETR) of the leaves showed that the transgenic plants had significantly higher parameters than those of WT plants, exhibiting a better photosynthetic performance (Fig. 6e-g). The better photosynthetic performance of *CmANR1*-transgenic plants gives a good explanation for their higher and more robust shoot growth.

To better explain the shoot developmental differences between transgenic and WT plants, we next evaluated the relative content of the main metabolites by a metabolomics analysis on the shoot parts of two kinds of plants. Similar to the root-metabolomics result, the OPLS-DA score plot and permutation test of both positive mode and negative mode data showed good stability and reliability in this study (Additional file 3). PCA score plots in ESI positive and negative mode based on HILIC UHPLC-Q-TOF MS data revealed a trend of separation between samples (Fig. 7a, b). Hierarchical clustering analysis showed an overview of the content differences and possible connections of the metabolites of transgenic and

wild-type shoots that were detected. The heat map and dendrograms showed choline and rhoifolin were clustered together in the positive mode, and both contents were increased, indicating the possible improvement in stress-resistance and pharmacological activities in shoots of transgenic plants. L-glutamate, L-asparagine and dihydrouracil were in closely clustered in the negative mode, which following their possible roles in amino acid metabolism (Fig. 7c, d). Regarding the relative content of the differently accumulated metabolites judged by the fold change in shoots, the situation was distinct from that of roots. Metabolites that were relevant to various amino acids metabolism, like L-glutamate, L-asparagine, and L-histidine were decreased in shoots of transgenic plants. The content of metabolites being involved in fatty or unsaturated fatty acids biosynthesis was significantly increased in shoots of transgenic plants, compared with that of WT plants. However, D-mannose and glycerol 3-phosphate, the main intermediates of nucleotide sugar metabolism and glycolysis, were 2.13- and 1.51-fold increased in shoots of transgenic plants compared with those of WT plants (Table 2). Taken together, we document here that over-expressing *CmANR1* could provoke considerable changes on both root and shoot development in chrysanthemum. *CmANR1* had pleiotropic positive effects on plant growth and development in chrysanthemum.

Discussion

Based on our previous reports, the current results provide further evidence that *CmANR1* has positive effects on root development in chrysanthemum. The *CmANR1*-transgenic plants have more robust root systems, such as longer and a greater number of LRs, ARs and root hairs, as well as a larger root system surface and volume, in comparison to WT plants (Fig. 1). We have observed and measured the root growth and developmental parameters of several periods of both transgenic and WT chrysanthemum (10-day-old tissue culture, 20-day-old tissue culture, and 40-day-old hydroponic culture), and it seemed that *CmANR1* could respond quickly to the higher concentration of nitrate (10 mM, under the culture condition) and its positive role in root development was obvious at the initial stage of growth, which might continue into the later growth and development in transgenic plants. On the other hand, in this study, we confirmed that *CmANR1*-transgenic plants grew much higher, were greener, had better photosynthetic performance than those of WT plants under the tissue-cultured conditions (Fig. 6). As *CmANR1*-overexpression in the transgenic plants was triggered by a *35S* promoter in our study, therefore, we could not determine whether the growth advantages of the transgenic plants on the shoot were due to the direct regulation of *CmANR1* on other molecular players in shoots or due to the indirect stimulative effect of more nutrients and water uptake by the more extensive root system of transgenic plants. More work is required to determine the possible mechanism underlying the root-shoot interaction in chrysanthemum.

Previous studies have reported that *ANR1* is a rapid nitrate-responsive and nitrate-dependent transcription factor gene [14, 28]. CmANR1 can act as a transcriptional activator of an auxin transport gene, thereby leading to auxin accumulation in roots during the nitrate signaling pathway in chrysanthemum [24]. Meanwhile, the *CmANR1*-overexpression conferred more nitrate uptake and more nitrate-contained in the roots of the transgenic plants (Fig. 3a). Apart from being as a signaling molecule, nitrate has its basic

nutritional role as the main nitrogen source for most land plants, and it will be taken up, translocated, assimilated and transitioned into other physiological compounds (such as amino acids) at the cellular level in the plants [37]. In our root metabolomics assay, it was clear that there were significant increases in the metabolites that were involved in various amino acid metabolisms in transgenic plants, such as L-histidine, L-pyroglutamic acid, 4-guanidinobutyric acid, and L-phenylalanine (Table 1). These findings suggest that *CmANR1* may have some influence on nitrate assimilation during root development under nitrate-rich conditions in chrysanthemum.

The TCA, well-known as an important central pathway connecting almost all metabolic pathways in plants, is responsible for the oxidation of respiratory substrates to drive ATP synthesis [38, 39]. Glycolysis, an oxidization process responsible for the conversion of glucose to pyruvic acid, is another ubiquitous cellular metabolism. Modifications of the expression of important kinases and mutases, such as hexokinase, pyruvate kinase, and phosphoglycerate mutase, could result in dramatic effects on photosynthetic metabolism [40]. Notably, metatranscriptomics analysis of roots showed DEGs and metabolites related to amino sugar and nucleotide sugar metabolism were mostly enriched. The detailed expression level manifested by fold changes of the genes being involved in glycolysis and TCA cycle were clearly illustrated. The result shows that the expressions of genes encoding hexokinase (TR12735|C1-g1, 1.119), pyruvate kinase (TR99|C0-g3, -1.075), and phosphoglycerate mutase-like (TR15403|C0-g1, 1.585) were significantly altered in transgenic plants (Fig. 4c, d). Moreover, the significant changes in the content of some respiration substrates, such as citrate, L-malic acid, maltotriose, and D-mannose, suggest a possible energy enhancement in the roots of transgenic plants, which might be another explanation for their better root system development. In conclusion, this evidence hints that there is a link between sugar metabolism and root development that is mediated by *CmANR1*.

Moreover, there were some other interesting metabolites accumulated in transgenic plants. First, choline was one of the most abundant metabolites in both roots and shoots of transgenic plants. Choline, as the primary source for acetyl choline (ACH), is also related to glycine, serine and threonine metabolism, and synthesis of glycine betaine (GlyBet) in the chloroplast [41]. ACH and GlyBet are essential for various important physiological processes and tolerance to abiotic stresses in plants [42, 43] .The increase in the content of choline gave some information on the possible amino acid transition enhancement and stresses-resistance improvement in transgenic plants, which provided a new idea for the future exploration. Second, rhoifolin, as one of the important flavonoids, has various significant biological activities, including anti-allergic, anti-inflammatory, antioxidant, antimicrobial, and anticancer effects [44]. In our shoot metabolomics assay, the content of rhoifolin showed a significant increase in transgenic plants, suggesting the possible improvement of the pharmacological value of on transgenic plants. Also, some metabolites that were closely related to the biosynthesis of unsaturated fatty acids and fatty acids, such as alpha-Linolenic acid, (4Z, 7Z, 10Z, 13Z, 16Z, 19Z)-4, 7, 10, 13, 16, 19-Docosahexaenoic acid, and cis-9-Palmitoleic acid, were found significantly increased in shoots of transgenic plants, suggesting the improvement of cold and disease resistance in transgenic plants.

In conclusion, we now present a working model of *CmANR1* on plant development (Fig. 8). In roots: *CmANR1* senses the higher nitrate signal passed by the sensor NRT1.1, which is located on the plasma membrane in roots. Then, CmANR1 formed a homodimer with another CmANR1, and a heterodimer with AGL21, trans-activating downstream target genes, such as auxin-related genes [24], sugar metabolism genes and nitrate responsive genes, resulting in changes in the related physiological processes in plants. The final increases of auxin [24], AAs, metabolites related to glycolysis, and TCA cycle in roots (Table 1) promoted root system development in chrysanthemum. Moreover, TF expression analysis suggested some TFs, such as NLPs, LBDs, and other MADS-box TFs, were more likely to act together with CmANR1 on root system development in this background (Fig. 5). Therefore, it can be concluded that *CmANR1* promoted root system development in chrysanthemum by combining the nitrate signaling pathway with auxin transport, nitrate assimilation, as well as glycolysis and the TCA cycle.

In shoots, the significant increases in shoot height, chlorophyll content, and three photosynthesis parameters (Pn, ETR, and ΦPSII) in transgenic plants indicated a more robust growth and better photosynthesis performance in the shoots of transgenic plants (Fig. 6). However, whether *CmANR1* directly exerted some effects on shoot development could not yet be determined. At the minimum, overexpression of *CmANR1* could trigger shoot development. Taken together, over-expressing *CmANR1* could prompt both root and shoot development in chrysanthemum.

Conclusion

In this study, we report that CmANR1 plays a positive role in root system development in chrysanthemum throughout the developmental stages of tissue culture. Metabolomics combined with transcriptomics assays show that CmANR1 promotes robust root system development by facilitating nitrate assimilation, and influencing the metabolic pathways of amino acid, glycolysis, and the tricarboxylic acid cycle (TCA) cycle. Also, we found that the expression levels of TFs associated with the nitrate signaling pathways, such as *AGL8*, *AGL21*, and *LBD29*, are significantly up-regulated in *CmANR1*-transgenic plants relative to the wild-type (WT) control; by contrast, the expression levels of *RHD3-LIKE*, *LBD37*, and *GATA23* were significantly down-regulated. These results suggest that these nitrate signaling associated TFs are involved in CmANR1-modulated control of root development. In addition, CmANR1 also acts as a positive regulator to control shoot growth and development. These findings provide potential mechanisms of MADS-box TF CmANR1 modulation of root and shoot development, which occurs by regulating a series of nitrate signaling associated TFs, and influencing the metabolic pathways of amino acid and glycolysis, as well as TCA cycle and nitrate assimilation.

Methods

Plant materials and growth conditions

The wild-type (WT) tissue cultured chrysanthemum were kindly provided by Professor Junping Gao (China Agricultural University). Dr. Cui-Hui Sun undertook the formal identification of the *CmANR1*-

transgenic chrysanthemum used in this study. Three independent *CmANR1*-transgenic lines (*CmANR1-OVX56*, *-OVX67*, and *-OVX81*) of chrysanthemum were generated by introducing a *35S::CmANR1-GFP* vector into chrysanthemum leaf discs via *Agrobacterium GV3101* [24]. *CmANR1*-transgenic and WT chrysanthemum were cultivated *in vitro* on Murashige and Skoog (MS) medium in a standardized culture room of Shandong Agricultural University. These materials have been deposited and publicly available in herbarium of Shandong Agricultural University. The deposit number is SDAU510008.

Morphological characterization of roots in chrysanthemum

About 10-day-old tissue-cultured chrysanthemum plants were used for root morphological characterization. Phenotype pictures of the root hairs on *CmANR1*-OVXs and WT chrysanthemum were photoed under optical microscope (Olympus CX31, Japan). Both the adventitious root (AR) number and root hair density of the plant materials were measured using Image J software (NIH, Bethesda, MD, USA). The length distribution of AR and root hair were calculated by the R Project Program (GNU, New Zealand).

RNA-Seq analysis

The high-quality RNA extraction for the roots of 10-day old transgenic and WT chrysanthemum (three biological replicates of each sample), library conduction, and RNA-Seq performed by the Illumina HiSeq2000 were carried out professionally by the Ori-gene Biotechnology Company (Ori-gene Inc, Beijing, China). The high-quality cleaned reads were assembled *de novo* into transcripts with default parameters according to a previous study [45]. The Unigenes were screened and functionally annotated with alignments to the GenBank non redundant (NR), UniProt (Swiss-Prot and TrEMBL), KOG, KEGG and Gene Ontology (GO) databases and *Arabidopsis* protein databases with a cut off E-value of 1e-5. GO terms were assigned and annotated as the previously described [46].

UHPLC/Q-TOF Settings

CmANR1-transgenic and WT chrysanthemum (six biological replicates of each sample) were used for metabolite profiling of roots and shoots. For metabolomics analysis, the sample separation was performed using an Agilent 1290 Infinity LC ultra-high pressure liquid chromatography (UHPLC) (Agilent, Palo Alto, USA) equipped with an electrospray ionization source operating in positive and negative ion modes. ACQUITY UPLC HSS T3 column (1.7 μm, 2.1 × 100 mm) was maintained at 25℃ with an eluotropic flow rate of 0.3 ml min^{-1}. The mobile phase A was composed of 25 mM ammonium acetate and 25 mM ammonium in water, and mobile phase B was 95% acetonitrile. The linear gradient elution was as follows: 0–1 min, 95% B; 1–14 min, 95% B–65% B; 14–16 min, 65% B–40%B; 16–18 min, 40% B, and 18–18.1 min, 40% B–95%.

The mass spectrometer (MS) was a Triple TOF 6600 system (AB SCIEX, Foster City, USA) with an electrospray (ESI) ionization source in positive (ESI^+) and negative (ESI^-) ion modes. The MS parameters were set as follows: scan m/z range: 60-1000 Da; product ion scan m/z range: 25-1000 Da; TOF MS scan accumulation time 0.2 s/spectra; product ion scan accumulation time 0.05 s/spectra; Ion Source Gas1 (Gas1), 60 psi; Ion Source Gas2 (Gas2), 60 psi; Curtain gas (CUR), 30 psi; source temperature 600℃; Ion

Sapary Voltage Floating (ISVF), ± 5500 V; MS/MS data were acquired in the information-dependent acquisition (IDA) and high sensitivity modes. Declustering potential (DP), ± 60 V; Collision energy, 35 ± 15 eV. IDA settings were exclude isotopes within 4 Da, and candidate ions to monitor per cycle 6.

Metabolomics data processing and analysis

The metabolomics raw data files were first converted into the .mzML format via ProteoWizard, and then, the converted data were imported into the XCMS software for peak alignment, correction of retention time, automatic integration, and extraction of the peak area with default parameter settings. The exact mass number match (< 25 ppm) and secondary spectral map matching mode were used for structure identification of metabolites, which were retrieved in a self-built laboratory database (Shanghai Applied Protein Technology, Inc., China). The data extracted by XCMS needed a further deletion of ion peaks, with, with > 50% missing values. Pattern recognition was conducted by SIMCA-P 14.1 software (Umetrics, Umea, Sweden). Statistical analysis was performed by MetaboAnalyst 2.0 (http://www.metaboanalyst.ca). Principle component analysis (PCA) and hierarchical clustering were used for the unsupervised multivariate statistical analysis after Pareto-scaling prepossessing of the data. Partial-least squares discrimination analysis (PLS-DA) was performed in a supervised method to identify the important variables with discriminative power. PLS-DA models were validated based on the multiple correlation coefficient (R^2) and cross-validated R^2 (Q^2) in cross-validation and permutation tests by applying 2000 iterations ($P > 0.001$). The significance of candidate metabolites was ranked using the variable importance in projection (VIP) score (> 1) from the PLS-DA model. For the univariate analysis, candidates were determined using Student's t-test statistics and multiple-fold analysis, comparing the means of WT group and the transgenic groups. The heat map in hierarchical clustering analysis was created using Metabo Analyst software (the distance was calculated using Pearson and the clustering using Ward).

Quantitative real-time PCR (RT-qPCR)

Total RNAs were extracted from roots of *CmANR1*-transgenic and WT chrysanthemum using TRIzol Reagent (Vazyme,Nanjing, China), followed by reverse transcription (RT) using a PrimeScript first-strand cDNA synthesis kit (TaKaRa, Dalian, China). The qPCR assay reaction procedure was referred to as Hu *et al* [47]. All reactions were performed in triplicate, and the chrysanthemum *Ubiquitin2* gene was used as an internal reference gene. The relative expression level of selected genes was calculated using the $2^{-\Delta\Delta Ct}$ method. The primers used for qPCR assays are listed in Additional file 5.

Chlorophyll analysis

Fresh leaves (~ 0.2 g) of chrysanthemum were cut into small pieces and ground using a little quartz sand and 2–3 mL 96% ethanol (v/v) until completely white. The chlorophyll-containing liquid was filtered and extracted in a total of 25 mL 96% ethanol. The extraction was measured using an ultraviolet spectrophotometer (U-5100, Hitachi, Japan) at A_{649}, A_{665}, and A_{470}. The chlorophyll contents were calculated according to the following formula: $Chla = 13.95A_{665} - 6.88A_{645}$; $Chlb = 24.96A_{649} - 7.32A_{665}$. The detailed operation procedure was referred to Hu *et al* [48].

Chlorophyll Fluorescence Parameters

Chlorophyll fluorescence was measured using a FMS-II plus modulated fluorometer (Hansatech, United Kingdom) on the same leaves from 10:00 AM to 1:00 PM. Minimal fluorescence (F_0), maximal fluorescence (F_m), PSII (determined as F_v/F_m), light-adapted maximum fluorescence (F_m'), and steady-state fluorescence yield (F_s) were measured and calculated referring` to the previous studies [49, 50]. The quantum efficiency of PSII (ΦPSII) was determined as (Fm'- Fs)/Fm' [51].

Statistical analysis

All samples were analyzed in triplicate and represented as the mean ± standard deviation unless specifically labeled. Significance analysis was performed using Student's *t* test. P-values ≤ 0.01 were considered to be significant, p-values ≤ 0.001 represented a very significant difference, and n.s. indicates no significant difference.

Abbreviations

WT
Wild-type; AR:Adventitious root; F_0:Minimal fluorescence; F_m:Maximal fluorescence; F_v/F_m:PSII; F_m':Light-adapted maximum fluorescence; F_s:Steady-state fluorescence yield

Declarations

Acknowlegements

We appreciated Prof. Zhi-long Bao at Shandong Agricultural University for constructive advice on paper writing, and thanked TopEdit (www.topeditsci.com) for its linguistic assistance during the preparation of this manuscript.

Funding

This work was supported by grants from the "National Key Research and Development Program" (2018YFD1000405), "Natural Science Foundation of Shandong Province" (ZR2019QC006), "National Natural Science Foundation of China" (31902049, 31972375). The construction of the experimental platform and purchase of experimental instruments in this work were funded by 2018YFD1000405. Material construction, metabolomics data and data analyses was financially supported by ZR2019QC006, 31902049, and 31972375.

Availability of data and materials

The datasets supporting the conclusions of this article are included within the article and its additional files. The *CmANR1* sequence is available at chrysanthemum genome database (http://www.amwayabrc.com/).

Authors' contributions

DGH and CHS conceived and designed the experiments. CHS, JHW, KDG, PZ, XYZ, and CSZ performed the experiments. CHS, DGH, and FM wrote the article. All authors read and approved the final manuscript.

Ethics approval and consent to participate

Not applicable.

Consent for publication

Not applicable.

Competing interests

The authors declare that they have no competing interests.

Publisher's Note

Springer Nature remains neutral with regard to jurisdictional claims in published maps and institutional affiliations.

Author details

National Key Laboratory of Crop Biology; MOA Key Laboratory of Horticultural Crop Biology and Germplasm Innovation; College of Horticulture Science and Engineering, Shandong Agricultural University, Tai'an, Shandong 271018, China

References

1. Lynch J. Root architecture and plant productivity. Plant Physiol. 1995;109:7–13.
2. Masclaux-Daubresse C, Daniel-Vedele F, Dechorgnat J, Chardon F, Gaufichon L, Suzuki A. Nitrogen uptake, assimilation and remobilization in plants: challenges for sustainable and productive agriculture. Bot. 2010;105:1141–1157.
3. Mitchum MG, Wang X, Davis EL. Diverse and conserved roles of CLE peptides. Curr. Opin. Plant Boil. 2008;11:75–81.
4. Rigal A, Yordanov YS, Perrone I, Karlberg A, Tisserant E, Bellini C. The AINTEGUMENTA LIKE1 homeotic transcription factor PtAIL1 controls the formation of adventitious root primordia in poplar. Plant Physiol. 2012;160:1996–2006.
5. Mohd-Radzman NA. Different pathways act downstream of the peptide receptor CRA2 to regulate lateral root and nodule development. Plant Physiol. 2016;171:2536–2548.
6. Bailey-Serres J, Bazin J. Emerging roles of long non-coding RNA in root developmental plasticity and regulation of phosphate homeostasis. Front. Plant Sci. 2015;6:400.

7. Sun CH, Yu JQ, Hu DG. Nitrate a crucial signal during lateral roots development. Front. Plant Sci. 2017;8:485.
8. Imin N, Nizamidin M, Wu T, Rolefe BG. Factors involved in root formation in Medicago truncatula. J. Exp. Bot. 2007;58:439–
9. Hao J, Tu LL, Tan JF, Deng FL, Tang WX, Nie YC. GbTCP, a cotton TCP transcription factor confers fibre elongation and root hair decampment by a complex regulating system, J. Exp. Bot. 2012;63:6267–6281.
10. Gutierrez L. Phenotypic plasticity of adventitious rooting in *Arabidopsis* is controlled by complex regulation of AUXIN RESPONSE FACTOR transcripts and microRNA abundance. Plant Cell. 2009;21:3119–3132.
11. Smaczniak C, Immink GH, Angenent GC, Kaufmann K. Developmental and evolutionary diversity of plant MADS domain factors: insights from recent studies. Development. 2012;139:3081–3098.
12. Zhang HM, Forde BG. An *Arabidopsis* MADS box gene that controls nutrient-induced changes in root architecture. Science. 1998;279:407–409.
13. Yu CY, Liu YH, Zhang AH. MADS-box transcription factor OsMADS25 regulates root development through affection of nitrate accumulation in rice. PLoS One. 2015;8:e0135196.
14. Gan Y, Bernreiter A, Filleur S, Abram B, Forde BG. Overexpressing the *ANR1* MADS-Box gene in transgenic plants provides new insights into its role in the nitrate regulation of root development. Plant Cell Physiol. 2012;53:1003–1016.
15. Farre's M, Pin'a B, Tauler R. LC-MS based metabolomics and chemometrics study of the toxic effects of copper on *Saccharomyce scerevisiae*. Metallomics. 2016;8:790–798.
16. Bhardwaj J, Chauhan R, Swarnkear MK, Chahota RK, Singh AK, Yadav SK. Comprehensive transcriptomic study on horse gram (*Macrotyloma uniflorum*): *De novo* assembly, functional characterization and comparative analysis in relation to drought stress. BMC Genomics. 2013;14:647.
17. Okazaki Y, Saito K. Integrated metabolomics and phytochemical genomics approaches for studies on rice. GigaScience. 2016;5:11.
18. Chan EK, Rowe FH, Hansen BG, Kliebenstein DJ. The complex genetic architecture of the metabolome. PLoS Genet. 2010;6:e1001198.
19. Nakabayashi R, Snaito K. Itegrated metabolomics for abiotic stress responses in plants. Curr. Opin. Plant Biol. 2015;24:10–16.
20. Watson BS, Bedair MF, Urbanczyk-Wochniak E, Huhman DV, Yang DS, Allen SN. Integrated metabolomics and transcriptomics reveal enhanced specialized metabolism in Medicago truncatula root border cells. Plant Physiol. 2015;167:1699–1716.
21. Xie YY, Luo D, Cheng YJ, Ma JF, Wang YM, Luo GA. Steaming-induced chemical transformations and holistic quality assessment of red ginseng derived from Panax ginseng by means of HPLC-ESI-MS/MSn-based multicomponent quantification fingerprint, J. Agric. Food Chem. 2012;60:8213–8224.

22. Wang H. UHPLC-Q-TOF/MS based plasma metabolomics reveals the metabolic perturbations by manganese exposure in rat models. Metallomics. 2017;9:192.
23. Luo J. Metabolite-based genome-wide association studies in plants. Curr. Opin. Plant Biol. 2015;24:31–
24. Sun CH, Yu JQ, Duan X, Wang JH, Zhang QY, Gu KD. The MADS transcription factor CmANR1 positively modulates root system development by directly regulating *CmPIN2* in chrysanthemum. Res. 2018;5:52.
25. Sangster T. A pragmatic and readily implemented quality control strategy for HPLC-MS and GC-MS based metabonomic analysis. Analyst. 2006;131:1075–1078.
26. Palenchar PM, Kouranov A, Lejay LV, Coruzzi GM. Genomewide patterns of carbon and nitrogen regulation of gene expression validate the combined carbon and nitrogen (CN)-signaling hypothesis in plants. Genome Biol. 2004;5:R91.
27. Marín IC, Loef I, Bartezko L, Searle I, Coupland G, Stitt M. Nitrate regulates floral induction in Arabidopsis, acting independently of light, gibberellin and autonomous pathways. Planta. 2011;233:539–552.
28. Sun CH, Yu JQ, Wen LZ, Guo YH, Sun X, Hao YJ, Hu DG, Zheng CS. Chrysanthemum MADS-box transcription factor CmANR1 modulates lateral root development via homo-/heterodimerization to influence auxin accumulation in Plant Sci. 2018;266:27–36.
29. Fan HM, Sun CH, Wen LZ, Liu BW, Ren H, Zheng CS. CmTCP20 Plays a Key Role in Nitrate and Auxin Signaling-Regulated Lateral Root Development in Chrysanthemum. Plant Cell Physiol. 2019;60:1581–1594.
30. Fan HM, Liu BW, Ma FF, Sun X, Zheng CS. Proteomic profiling of root system development proteins in chrysanthemum overexpressing the *CmTCP20* Plant Sci. 2019;287:110175.
31. Rubin G. Members of the LBD Family of Transcription Factors Repress Anthocyanin Synthesis and Affect Additional Nitrogen Responses in Plant Cell. 2009;21:3567–3584.
32. Rybel BD, Vassieva V, Parizot B, Demeuleaere M. A Novel Aux/IAA28 Signaling Cascade Activates GATA23-Dependent Specification of Lateral Root Founder Cell Identity. Biol. 2010;20:1697–1706.
33. Trupiano D, Yordanov Y, Regan S, Meilan R. Identification, characterization of an AP2/ERF transcription factor that promotes adventitious, lateral root formation in Populus. Planta. 2013;238:271–282.
34. Guan PZ, Ripoll JJ, Wang RH, Vuong L, Bailey-Steinitz LJ. Interacting TCP and NLP transcription factors control plant responses to nitrate availability. 2017;114:2419–2424.
35. Yu LH, Miao ZQ, Qi GF. MADS-Box transcription factor AGL21 regulates lateral root development and responds to multiple external and physiological signals. Plant. 2014;11:1653–1669.
36. Gan Y, Filleur S, Rahman A, Gotensparre S, Forde BG. Nutritional regulation of ANR1 and other root expressed MADS-box genes in *Arabidopsis thaliana.* 2005;222:730–742.

37. Bouguyon E, Gojon A, Nacry P. Nitrate sensing and signaling in plants. Seminars Cell Dev. Biol. 2012;23:648–654.
38. Sweetlove LJ, Beard KFM, Nunes A. Not just a circle: flux modes in the plant TCA cycle. Trends Plant Sci. 2010;15:462–470.
39. Akram M. Citric Acid Cycle and Role of its Intermediates in Metabolism. Cell Biophys. 2014;68:475–478.
40. Fernie AR, Carrari F, Sweetlove LJ. Respiratory metabolism: glycolysis, the TCA cycle and mitochondrial electron transport. Opin. Plant Biol. 2004;7:254–261.
41. Nuccio ML, McNeil SD, Ziemak MJ, Hanson AD, Jain RK, Selvaj G. Choline Import into Chloroplasts Limits Glycine Betaine Synthesis in Tobacco: Analysis of Plants Engineered with a Chloroplastic or a Cytosolic Pathway. Metabolic Engineering. 2000;2:300–
42. Zhang HM, Murzello C, Sun Y, Kim M, Xie XT, Jeter RM. Choline and Osmotic-Stress Tolerance Induced in *Arabidopsis* by the Soil Microbe Bacillus subtilis (GB03). MPMI. 2010;8:1097–1104.
43. Yamamoto K, Sakamoto H, Momonoki YS. Maize acetylcholinesterase is a positive regulator of heat tolerance in plants. Plant Physiol. 2011;168:1987–1992.
44. Refaat J. A review of sources and biological activities. IJP. 2015;2:102–109.
45. Grabherr MG, Hass BJ, Yassour M, Levin JZ. Full-length transcriptome assembly from RNA-Seq data without a reference genome. Nat. Biotechnol. 2011;29:644–652.
46. Hu DG, Yu JQ, Han PL, Xie XB, Sun CH, Hao YJ. The regulatory module MdPUB29-MdbHLH3 connects ethylene biosynthesis with fruit quality in apple. New Phytol. 2019; 221:1966–1982.
47. Hu DG, Sun CH, Ma QJ, You CX, Cheng LL, Hao YJ. MdMYB1 regulates anthocyanin and malate accumulation by directly facilitating their transport into vacuoles in apples. Plant Physiol. 2016;170:1315–1330.
48. Hu DG, Sun CH, Gu KD, Hao YJ. The basic helix-loop-helix transcription factor MdbHLH3 modulates leaf senescence in apple via the regulation of dehydratase-enolase-phosphatase complex 1. Hortic. Res. 2020;7:1–6.
49. Wang H, Liu R, Jin J. Effects of zinc and soil moisture on photosynthetic rate and chlorophyll fluorescence parameters of maize. Biol. Plantarum. 2009;53:191–
50. Wang H, Jin J. Photosynthetic rate, chlorophyll fluorescenceparameters, and lipid peroxidation of maize leaves as affected by zinc deficiency. Photosynthetica. 2005;43:591–
51. Genty B, Briantais J, Baker N. The relationship between the quantum yields of photosynthetic electron transport and photo-chemical quenching of chlorophyll fluorescence. Biophys. Acta. 1989;990:87-92.

Tables

Due to technical limitations, table 1-2 is only available as a download in the Supplemental Files section.

Figures

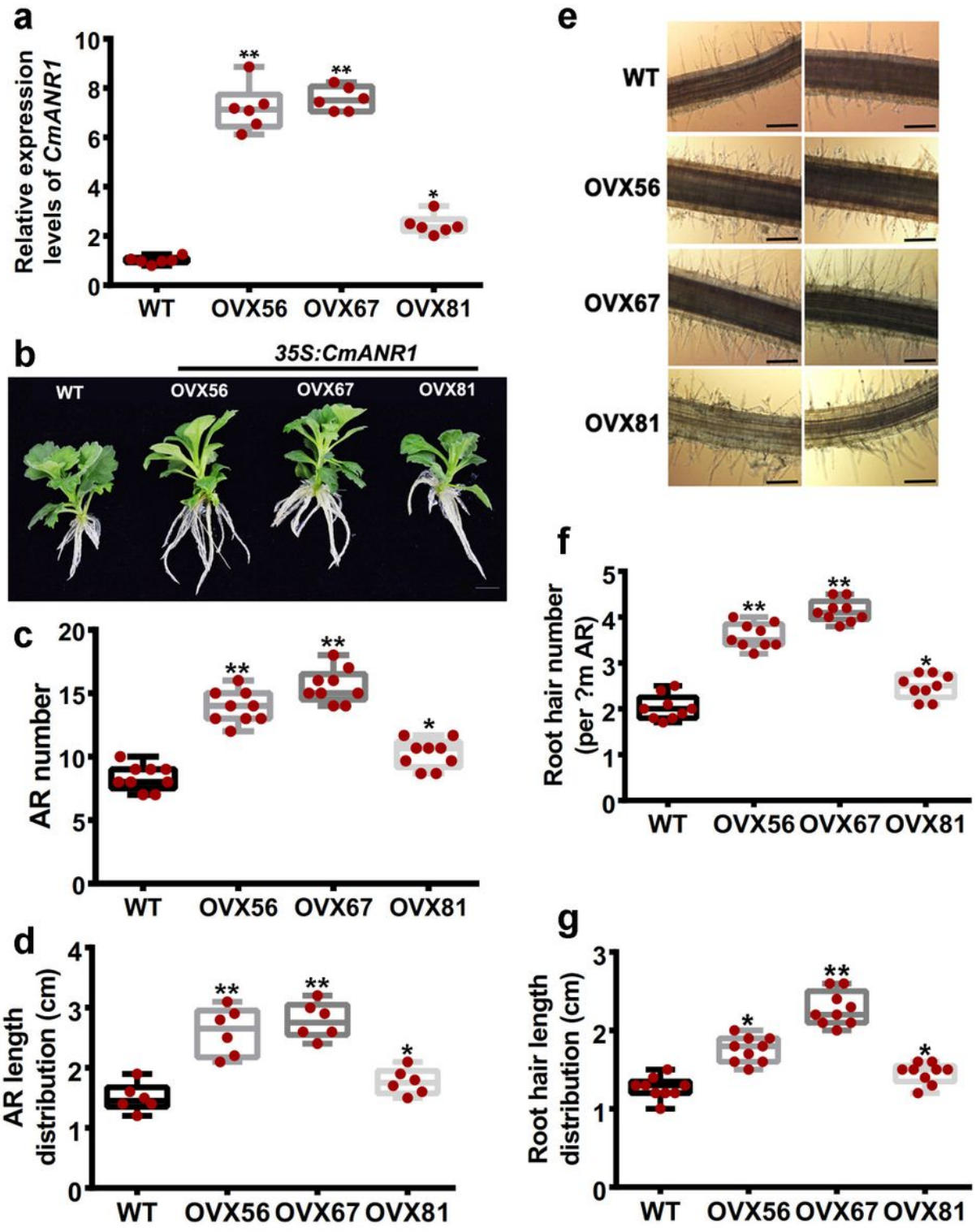

Figure 1

CmANR1 promotes adventitious root (AR) and hair root development in chrysanthemum. a Relative expression of CmANR1 in three CmANR1-overexpressing (OVXs) and wild-type (WT) chrysanthemum lines. b Phenotype of CmANR1-overexpressing (OVXs) and WT chrysanthemum (10 day-old, tissue-

cultured). Scale bar = 1 cm. c, d AR number (c) and AR length distribution (d) of CmANR1-OVXs and WT chrysanthemum. e Phenotype of root hair on CmANR1-OVXs and WT chrysanthemum. Scale bar = 40 μm. f, g Hair root density (f) and length distribution (g) of CmANR1-OVXs and WT chrysanthemum. Statistical significance was determined using Student's t-test. No significance (n.s.): $p > 0.01$; *$p < 0.01$; **$p < 0.001$.

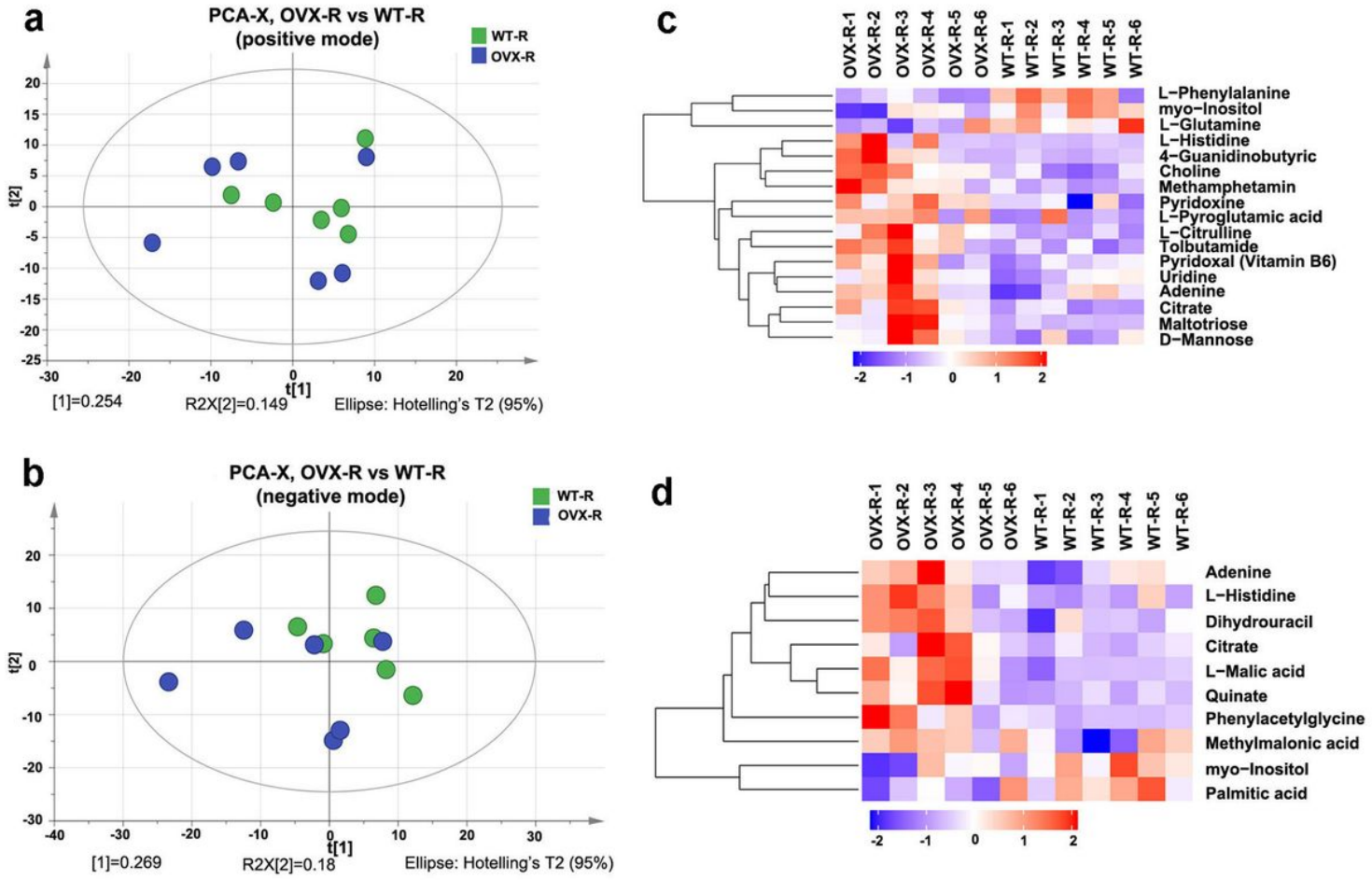

Figure 2

Principal component analysis (PCA) score plots and hierarchical clustering of the metabolites in roots. PCA score plots in ESI positive mode (a) and negative mode (b) based on HILIC UHPLC-Q-TOF MS data of root samples of CmANR1-OVXs and WT chrysanthemum. Hierarchical clustering results of significantly different metabolites of positive (c) and negative mode (d) data of roots in CmANR1-OVXs and WT chrysanthemum.

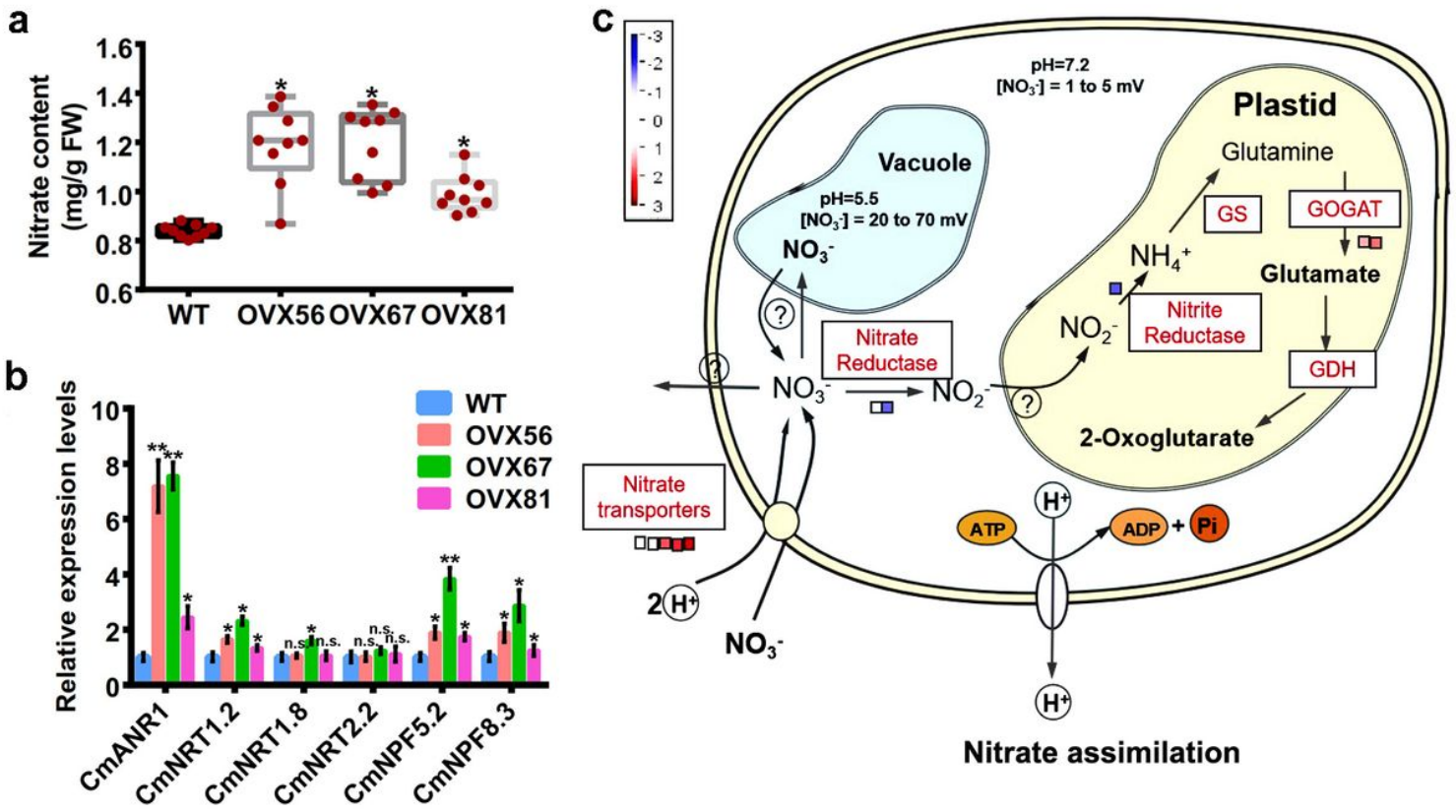

Figure 3

CmANR1 motivates nitrate assimilation in roots of chrysanthemum. a Nitrate content in roots of CmANR1-transgenic and WT chrysanthemum. b Relative expression level of several nitrate/peptide transporter genes in roots of CmANR1-transgenic and WT chrysanthemum. c The differently expressed genes (DEGs) during nitrate assimilation in roots. Data are shown as the mean ± SE based on three or more replicates. Statistical significance was determined using Student's t-test. n.s.: $p > 0.01$; *$p < 0.01$; **$p < 0.001$.

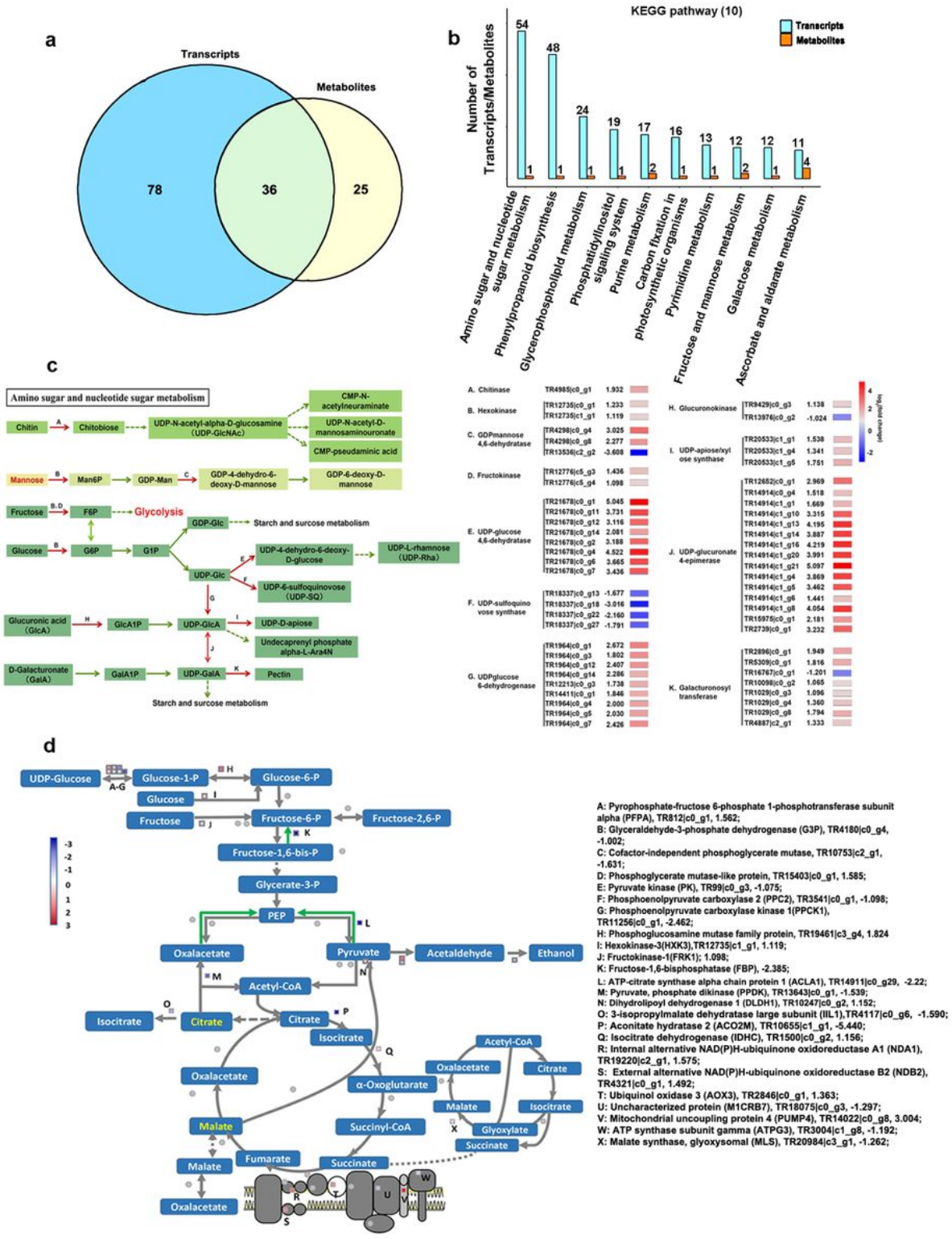

Figure 4

Metabolomic and transcriptomic conjoint analysis of roots in CmANR1-trangenic and WT chrysanthemum. a Venn diagram of significant differential transcripts and metabolites that were involved in same metabolic pathways in roots of chrysanthemum. b The same KEGG pathways (top10) shared by transcriptomic and metabolomic data of roots in chrysanthemum. c The representative metabolic pathways and related DEGs that were involved in Amino sugar and nucleotide sugar metabolism. Red

arrows suggest where the DEGs function. The log2(fold change) and heat meap of the related DEGs in OVXs/WT are listed on the left. d The changing metabolites and DEGs being involved in Glycolysis and TCA cycle in CmANR1-OVXs chrysanthemum.

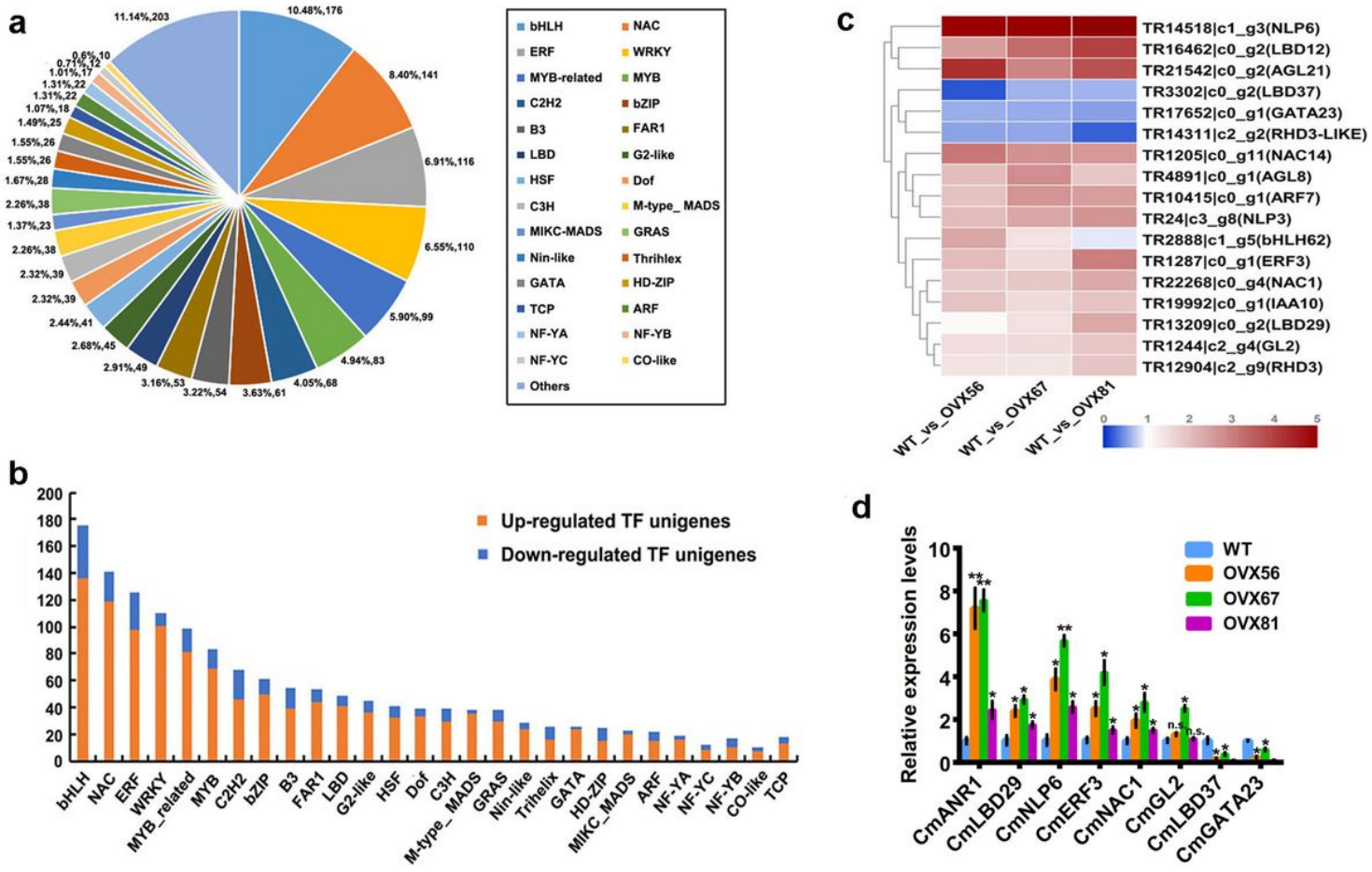

Figure 5

The DEGs annotated as transcription factors (TFs) in the chrysanthemum transcriptome. a Number and percentage of TF unigenes of DEGs in chrysanthemum transcriptome. b Numbers of up-/down-regulated TF unigenes of DEGs in chrysanthemum transcriptome. c The heatmap of TF unigenes related to root/root hair development between CmANR1-OVXs and WT. d The relative expression level of several TF genes related to root/ root hair development in chrysanthemum. Data are shown as the mean ± SE based on three or more replicates. Statistical significance was determined using Student's t-test. n.s.: $p > 0.01$; *$p < 0.01$; **$p < 0.001$.

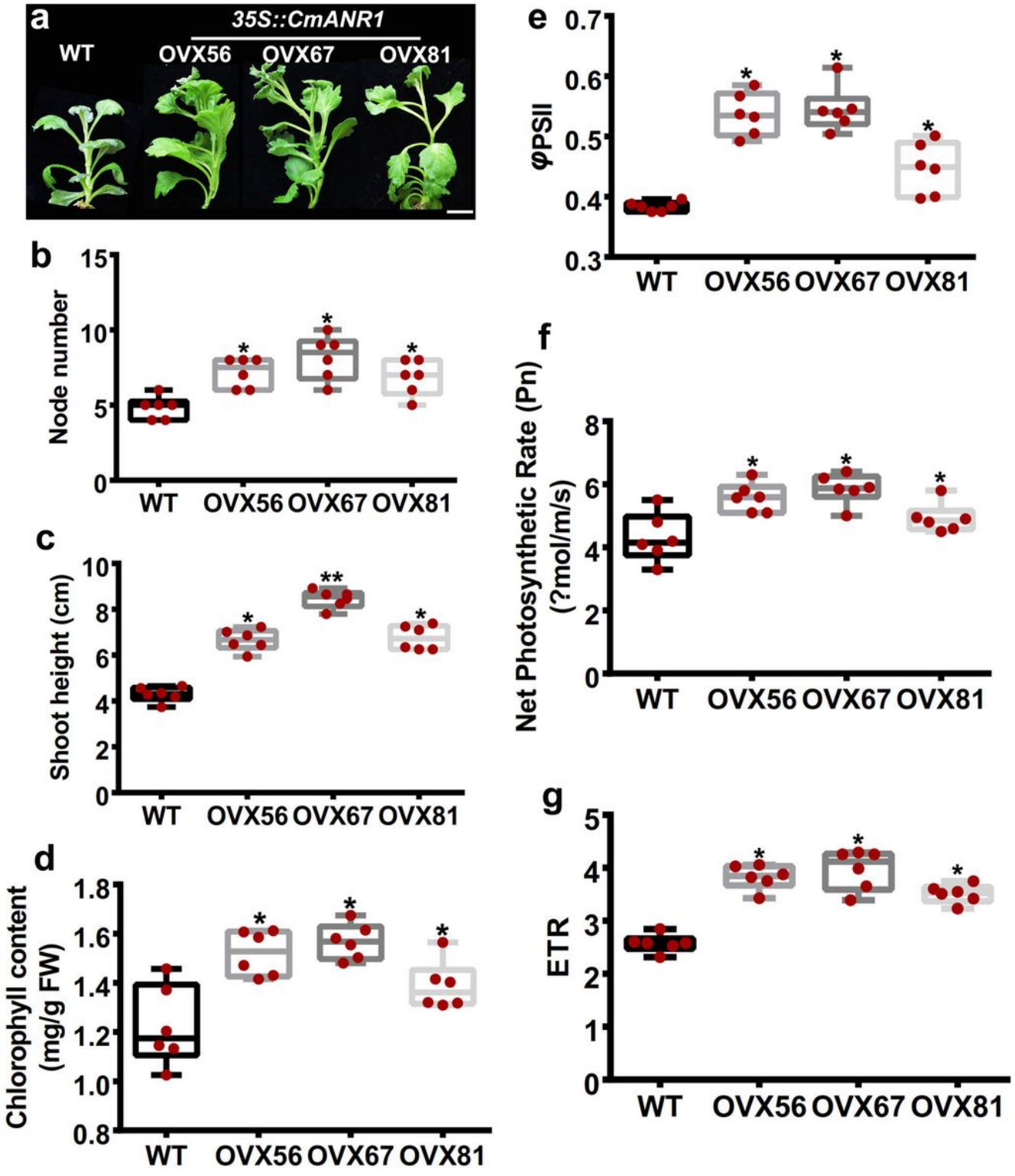

Figure 6

CmANR1-overexpressing improves shoot growth and photosynthesis in chrysanthemum. a The phenotype of shoots in WT and CmANR1-OVXs plants. (20 day-old, tissue-cultured). Scale bar = 1 cm. b, c The node number (b) and shoot height (c) of WT and CmANR1-OVXs plants. d The chlorophyll content in mature leaves of transgenic and wild-type chrysanthemum. e-g Actual photochemical efficiency (ΦPSII) (e), net photosynthetic rate (Pn) (f), and electron transfer rate (ETR) (g) of leaves of transgenic and wild-

type chrysanthemum. The data represent the means ± SE of three independent experiments. Statistical significance was determined using Student's t-test. No(n.s.): p > 0.01; *p < 0.01; **p < 0.001.

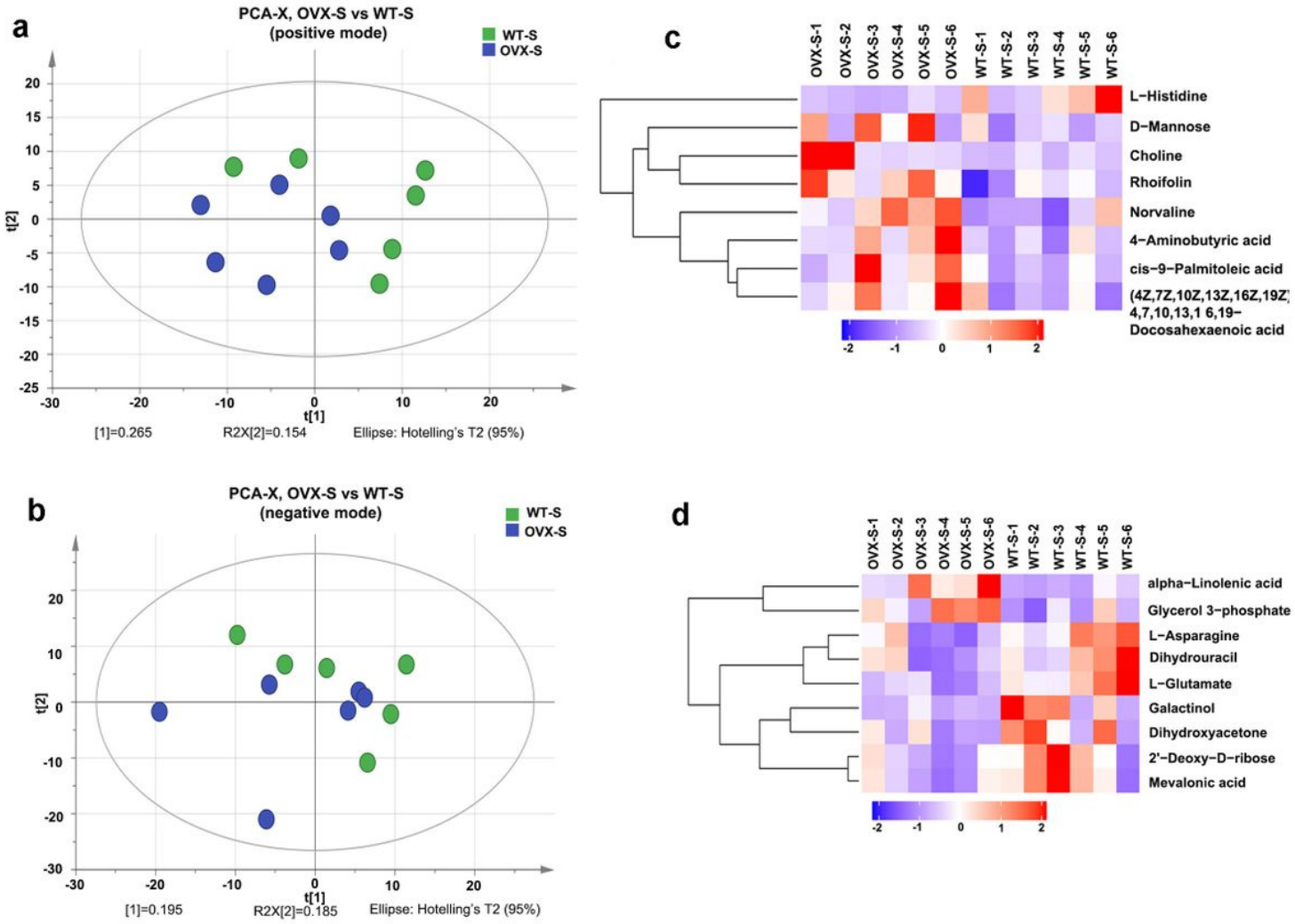

Figure 7

Principal component analysis (PCA) score plots and hierarchical clustering of the metabolites in shoots. PCA score plots in ESI positive mode (a) and negative mode (b) based on HILIC UHPLC-Q-TOF MS data of shoot samples of CmANR1-OVXs and WT chrysanthemum. Hierarchical clustering result of differently accumulated metabolites of positive (c) and negative mode (d) data of shoots in CmANR1-OVXs and WT chrysanthemum.

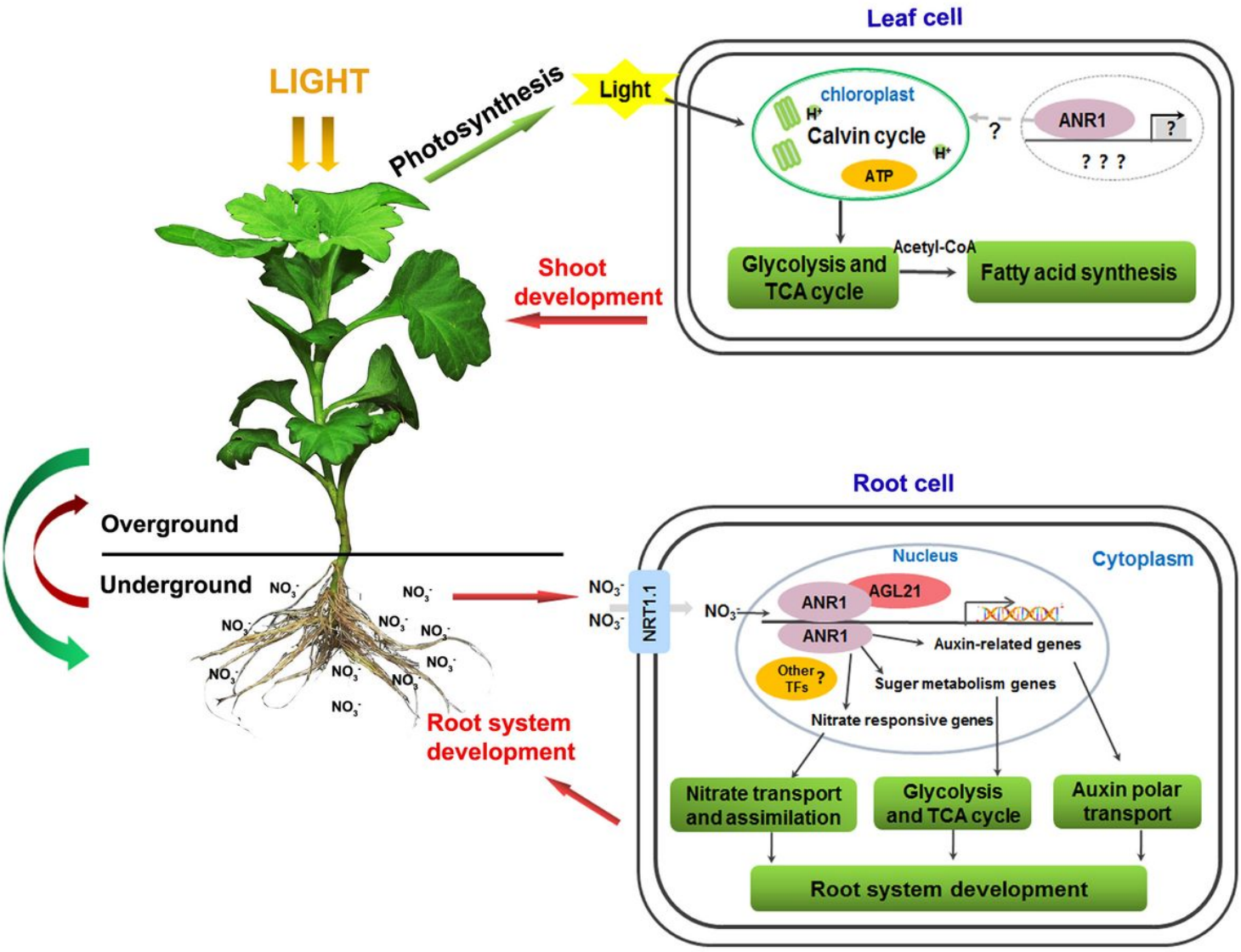

Figure 8

The conclusion of the CmANR1 working model on both root and shoot development in chrysanthemum.

Supplementary Files

This is a list of supplementary files associated with this preprint. Click to download.

- Additionalfiles.doc
- Table2.pdf
- Table1.pdf